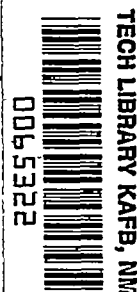


NACA TN 1963

8393



NATIONAL ADVISORY COMMITTEE FOR AERONAUTICS

TECHNICAL NOTE 1963

STRESSES IN AND GENERAL INSTABILITY OF
MONOCOQUE CYLINDERS WITH CUTOUTS
VIII - CALCULATION OF THE BUCKLING LOAD OF CYLINDERS WITH
LONG SYMMETRIC CUTOUT SUBJECTED TO PURE BENDING

By N. J. Hoff, Bruno A. Boley, and Mervin W. Mandel

Polytechnic Institute of Brooklyn



Washington
October 1949



NATIONAL ADVISORY COMMITTEE FOR AERONAUTICS

TECHNICAL NOTE 1963

STRESSES IN AND GENERAL INSTABILITY OF
MONOCOQUE CYLINDERS WITH CUTOUTSVIII - CALCULATION OF THE BUCKLING LOAD OF CYLINDERS WITH
LONG SYMMETRIC CUTOUT SUBJECTED TO PURE BENDING

By N. J. Hoff, Bruno A. Boley, and Mervin W. Mandel

SUMMARY

A strain-energy theory similar to one developed earlier at PIBAL (Polytechnic Institute of Brooklyn Aeronautical Laboratories) was established for the calculation of the buckling load in pure bending of reinforced monocoque cylinders which have a symmetric cutout on the compression side and buckle according to general-instability patterns. The difference between the present and the earlier theories is the use of the axial wave length as an additional parameter whose value was determined from a minimum condition. The theory was applied to four cylinders which were tested earlier at PIBAL. Fair agreement was found between theory and the results of the experiments.

INTRODUCTION

Reinforced monocoque cylinders are subject to failure by a simultaneous buckling of frames, stringers, and sheet covering. This type of failure is known as general instability. The problem of the general instability of reinforced circular cylinders subjected to pure bending has been investigated in some detail by various authors (references 1 to 13). These papers have dealt with complete cylinders, cylinders having symmetric cutouts on the compression side, and cylinders having side cutouts.

Reference 12 presents a strain-energy theory and the results of calculations for the buckling load of cylinders having a short symmetric cutout on the compression side. In the theory it was assumed that the general-instability bulge had the same wave length as the cutout.

In this paper the general-instability buckling load of cylinders having long symmetric cutouts on the compression side is calculated by

strain-energy methods. The axial wave length of the bulge is used as a parameter whose magnitude is found from the requirement that the buckling load be a minimum. Thus it is possible to determine whether the axial wave length is the same as the length of the cutout.

Test results showed that for some cylinders the bulge appeared to be antisymmetric with respect to the vertical plane of symmetry of the cylinder perpendicular to the axis. Therefore the calculations were carried out for the two different assumptions of deflected shape at buckling, one longitudinally symmetric, the other antisymmetric.

In both assumptions for the shape of the bulge, the displacements at buckling were represented by the first seven terms of a Fourier series in the circumferential direction and by a few terms of a trigonometric series in the axial direction. In the case of longitudinal symmetry, the trigonometric series in x consisted of sine power terms and contained a parameter which had to be determined from the minimum buckling load condition. For longitudinal antisymmetry the series was a Fourier sine series in x which also contained a parameter. Boundary conditions were used to determine four of the seven coefficients of the Fourier series in ϕ for the circumferential variation of the shape while one remained undetermined as in all buckling problems. The remaining two coefficients as well as the circumferential wave length were calculated from the minimum buckling load requirement.

The strain energies considered were those due to bending of the rings in their own plane, radial and tangential bending as well as torsion of the stringers, and shear in the sheet. The extensional strain energy of the sheet was accounted for by adding an effective width of sheet to the rings and stringers. The external work was calculated on the assumption of a linear force distribution in the stringers, which is in better agreement with test results (reference 9) than a linear stress or strain distribution.

The buckling load was calculated from the requirement that the strain energy corresponding to the transition from the unbuckled into the buckled shape be equal to the work done by the applied loads. The minimum value of the buckling load was found by assuming the circumferential wave length equal to some integral number of stringer fields, the axial wave length equal to some integral number of ring fields, and a numerical value for the parameter in the axial variation of the shape. The values of the two undetermined Fourier coefficients were calculated so as to make the buckling load a minimum, and with these two coefficients fixed the value of the axial parameter was calculated in a similar manner. The process was repeated until the three parameters reached steady values and the buckling load became a minimum. This value of the buckling load was compared with values obtained from other assumptions of axial and circumferential wave lengths and the lowest load was taken as the absolute minimum buckling load of the cylinder.

For his substantial share in the numerical work the authors are indebted to Mr. Leon Kaplan. The investigation was conducted under the sponsorship and with the financial assistance of the National Advisory Committee for Aeronautics.

SYMBOLS

a, a_0, a_1, a_2, a_3	Fourier coefficients
A, A_{eff}	cross-sectional area of stringer plus effective width of sheet
b, b_1, b_2, b_3	Fourier coefficients
c	parameter
C	geometric coefficient in torsional rigidity GC
d	width of panel measured along circumference
e	parameter
E	Young's modulus
E_{tan}	tangent modulus
E_{red}	reduced modulus
G	shear modulus
G_0	shear modulus of sheet covering at zero compressive load
G_{eff}	effective shear modulus
h	width of stringer
i	index indicating position along circumference
I_r	moment of inertia of ring section and its effective width of sheet for bending in its own plane
I_{str_r}	moment of inertia of stringer section and its effective width of sheet for bending in the radial direction (about a tangential axis)

I_{str_t}	moment of inertia of stringer section and its effective width of sheet for bending in the tangential direction (about a radial axis)
j	index indicating position along axial direction
L	length of bulge in axial direction
L_1	distance between adjacent rings
m	number of rings involved in bulge
$m + 1$	number of ring fields involved in bulge
M	applied bending moment; function of n , a , and b , appearing in strain energy of bending in rings
M_{cr}	applied bending moment at buckling
n	parameter defining length of bulge in circumferential direction
P_1, P_2	polynomial functions of a and b
P_{cr}	force in one of the stringers at edge of cutout at buckling
P_i	force in i th stringer
Q	function of x and c or e appearing in shear strain energy
r	radius of cylinder
R	function of n , ϕ , a , and b appearing in shear strain energy
s	number of stringers involved in one-half of bulge
S	total number of stringers in cylinder
t	thickness of sheet covering
U	strain energy
U_r	strain energy stored in rings because of bending of rings in their own plane

U_{str_r}	strain energy stored in stringers because of bending about a tangential axis
U_{str_t}	strain energy stored in stringers because of bending about a radial axis
U_t	strain energy stored in stringers because of torsion
U_{sh}	strain energy stored in sheet covering because of shear
$2w$	effective width of sheet
w_n	rotation of tangent to ring
w_r	radial displacement of a point on a ring or a stringer
w_t	tangential displacement of a point on a ring or a stringer
W	work done by external forces
x	coordinate measuring distance along axis of cylinder
2α	cutout angle
$\alpha_n, \alpha_r, \alpha_t$	coefficients used in calculation of shear strain in a panel due to rotations and displacements of its corners
γ	shear strain
δ	distance of neutral axis from horizontal diameter of cylinder
ϵ	normal strain in a stringer
ϵ_{cr}	buckling strain of a panel of sheet covering
ϕ	angular coordinate measuring circumferential distance from edge of cutout
ϕ_r'	function of $n, \phi, a,$ and b appearing in expression for w_n
ϕ_r	function of $n, \phi, a,$ and b appearing in expression for w_r
ϕ_t	function of $n, \phi, a,$ and b appearing in expression for w_t

THE DEFLECTED SHAPE

The shape of the bulge at buckling is determined mainly by the radial deflections. It was observed in experiments conducted on cylinders designed to fail by general instability that, while most of the cylinders failed in a longitudinally symmetric bulge, there were some specimens which failed in what appeared to be a longitudinally antisymmetric bulge pattern (reference 14). For that reason, these two types of deflected shape were considered. Typical deflection patterns of stringers and a ring are shown in figure 1.

SYMMETRIC DEFLECTION PATTERN

The expression chosen to represent the radial deflections that are symmetric longitudinally is:

$$w_r = \left[\sin^2(\pi x/L) + c \sin^6(\pi x/L) \right] \phi_r \quad (1)$$

where

$$\begin{aligned} \phi_r = & \left(a_0 + a_1 \cos n\varphi + a_2 \cos 2n\varphi + a_3 \cos 3n\varphi + \right. \\ & \left. b_1 \sin n\varphi + b_2 \sin 2n\varphi + b_3 \sin 3n\varphi \right) \end{aligned} \quad (1a)$$

provided

$$0 \leq \varphi \leq \pi/n$$

$$0 \leq x \leq L$$

Also,

$$w_r = 0$$

for $\varphi > \pi/n$ and/or $x < 0, x > L$. The notation and sign convention are shown in figure 2.

The deformations of the rings were assumed to be inextensional. The condition for inextensional deformations is:

$$w_r = -\partial w_t / \partial \varphi \quad (2)$$

Therefore the tangential deformations are given by:

$$w_t = [\sin^2(\pi x/L) + c \sin^6(\pi x/L)] \Phi_t \quad (3)$$

where

$$\begin{aligned} \Phi_t = -(1/n) & \left[a_0 \varphi + a_1 \sin n\varphi + (a_2/2) \sin 2n\varphi + (a_3/3) \sin 3n\varphi - \right. \\ & \left. b_1 \cos n\varphi - (b_2/2) \cos 2n\varphi - (b_3/3) \cos 3n\varphi \right] \end{aligned} \quad (3a)$$

provided

$$0 \leq \varphi \leq \pi/n$$

$$0 \leq x \leq L$$

Also,

$$w_t = 0$$

when $\varphi > \pi/n$ and/or $x < 0$, $x > L$. The arbitrary function of x which would normally appear in equation (3) as a result of the integration of equation (2) is zero if the displacements are symmetric about a vertical diameter.

If it is required that there be a smooth transition between the bulge and the undistorted part of the cylinder at $\varphi = \pi/n$, then:

(1) The tangential displacements must vanish:

$$w_t = 0 \quad (4a)$$

when $\varphi = \pi/n$ for all values of x

(2) The radial displacements must vanish:

$$w_r = 0 \quad (4b)$$

when $\varphi = \pi/n$ for all values of x

(3) There must be no sudden change in the direction of the tangent:

$$\partial w_r / \partial \varphi = 0 \quad (4c)$$

when $\varphi = \pi/n$ for all values of x

(4) There must be no sudden change in the curvature:

$$\partial^2 w_r / \partial \varphi^2 = 0 \quad (4d)$$

when $\varphi = \pi/n$ for all values of x . Also, in order to have a smooth transition between the bulge and the undistorted part of the cylinder at $x = 0$ and/or $x = L$:

(5) The tangential displacements must vanish:

$$w_t = 0 \quad (4e)$$

when $x = 0$ or L for all values of φ

(6) The radial displacements must vanish:

$$w_r = 0 \quad (4f)$$

when $x = 0$ or L for all values of φ

(7) There must be no sudden change in the direction of the tangent:

$$\partial w_r / \partial x = 0 \quad (4g)$$

when $x = 0$ or L for all values of φ . Conditions (5), (6), and (7) are automatically satisfied by the expressions in the assumed deflected shape for all values of the parameter c . The remaining four conditions establish four relationships between the Fourier coefficients and make it possible to determine any four of the coefficients in terms of the remaining three. If a_0 , a_1 , and b_1 are retained as the basic parameters, and the notation

$$\left. \begin{aligned} a_1/a_0 &= a \\ b_1/a_0 &= b \end{aligned} \right\} \quad (5)$$

is used, then equations (1a) and (3a) become:

$$\begin{aligned} w_r = a_0 & \left[\sin^2(\pi x/L) + c \sin^6(\pi x/L) \right] \left[1 + a \cos n\varphi + (1.6a - 1.8) \cos 2n\varphi + \right. \\ & (0.6a - 0.8) \cos 3n\varphi + b \sin n\varphi + (3.2b + 3.6\pi) \sin 2n\varphi + \\ & \left. (1.8b + 2.4\pi) \sin 3n\varphi \right] \end{aligned} \quad (6)$$

$$\begin{aligned}
 w_t = & -(a_0/n) [\sin^2(\pi x/L) + c \sin^6(\pi x/L)] [n\phi + a \sin n\phi + \\
 & (0.8a - 0.9) \sin 2n\phi + (0.2a - 0.2666 \dots) \sin 3n\phi - \\
 & b \cos n\phi - (1.6b + 1.8\pi) \cos 2n\phi - (0.6b + 0.8\pi) \cos 3n\phi] \quad (7)
 \end{aligned}$$

CALCULATION OF STRAIN ENERGY FOR THE
SYMMETRIC DEFLECTED SHAPE

Strain Energy Stored in Rings

The strain energy stored in one-half of any one ring is:

$$U = (EI_r/2r^3) \int_0^{\pi/n} \left[w_r + \left(\partial^2 w_r / \partial \phi^2 \right) \right]^2 d\phi \quad (8)$$

If the value of w_r is substituted from equation (6) and the strain energy is summed up over all the rings, the following expression is obtained:

$$\begin{aligned}
 U_r = (1/2) \sum_{j=1}^m (EI_r/r^3) & [\sin^2(\pi j/L) + \\
 c \sin^6(\pi j/L)]^2 & \int_0^{\pi/n} \left[\phi_r^2 + \left(\partial^2 \phi_r / \partial \phi^2 \right) \right]^2 d\phi \quad (9)
 \end{aligned}$$

where m is the total number of rings included in the wave length L . The integration yields a result in closed form. If all the rings have the same bending rigidity EI_r , the total strain energy for one-half of the cylinder is:

$$U_r = (a_0^2/2r^3)(EI_r M) \sum_{j=1}^m \left[\sin^2(\pi j/L) + c \sin^6(\pi j/L) \right]^2 \quad (10)$$

where

$$\begin{aligned}
 nM = & \left[\pi + 10.053096(1 - 9n^2) + 206.01005(1 - 4n^2)^2 + \right. \\
 & 90.303387(1 - 9n^2)^2 - 18.095573(1 - 4n^2)(1 - 9n^2) \left. \right] + \\
 & a \left[-9.0477868(1 - 4n^2)^2 - 1.5079645(1 - 9n^2)^2 + \right. \\
 & 30.159289(1 - n^2)(1 - 4n^2) + 18.095573(1 - 4n^2)(1 - 9n^2) \left. \right] + \\
 & b \left[4(1 - n^2) + 2.4(1 - 9n^2) + 113.69784(1 - 4n^2)^2 + \right. \\
 & 42.636690(1 - 9n^2)^2 + 2.4(1 - n^2)(1 - 4n^2) - \\
 & 3.68(1 - 4n^2)(1 - 9n^2) \left. \right] + a^2 \left[(\pi/2)(1 - n^2)^2 + 4.0212386(1 - 4n^2)^2 + \right. \\
 & 0.5654867(1 - 9n^2)^2 \left. \right] + b^2 \left[(\pi/2)(1 - n^2)^2 + 16.084954(1 - 4n^2)^2 + \right. \\
 & 5.08938(1 - 9n^2)^2 \left. \right] + ab \left[6.4(1 - n^2)(1 - 4n^2) + \right. \\
 & 3.84(1 - 4n^2)(1 - 9n^2) \left. \right] \quad (11)
 \end{aligned}$$

It is possible but cumbersome to sum up in closed form the trigonometric functions describing the deflected shape in the axial direction as given in equation (10). It was found more convenient to carry out the summation numerically.

Strain Energy Stored in Stringers

The strain energy stored in the stringers because of bending in the radial direction is:

$$U_{\text{str}_r} = (1/2) \sum_1 EI_{\text{str}_r} \int_0^L \left(\partial^2 w_r / \partial x^2 \right)^2 dx \quad (12)$$

where the summation is extended over all the stringers involved in the bulge in one-half the cylinder. Substitution of the value of w_r from equation (6) into equation (12) and integration gives:

$$\begin{aligned}
U_{\text{str}_r} &= (1/2) \sum_1 EI_{\text{str}_r} (\phi_r)^2 (\pi/L)^4 \int_0^L \left[2 \cos^2(\pi x/L) - 2 \sin^2(\pi x/L) + \right. \\
&\quad \left. 30c \sin^4(\pi x/L) \cos^2(\pi x/L) - 6c \sin^6(\pi x/L) \right]^2 dx \\
U_{\text{str}_r} &= (\pi^4/L^3) \left[1 + (15/8)c + (441/128)c^2 \right] \sum_1 EI_{\text{str}_r} (\phi_r)^2 \quad (13)
\end{aligned}$$

The strain energy stored in the stringers because of bending in the tangential direction is:

$$U_{\text{str}_t} = (1/2) \sum_1 EI_{\text{str}_t} \int_0^L (\partial^2 w_t / \partial x^2)^2 dx \quad (14)$$

where the summation is extended over all the stringers involved in the bulge in one-half of the cylinder. With the aid of equation (7) this strain energy becomes:

$$U_{\text{str}_t} = (\pi^4/L^3) \left[1 + (15/8)c + (441/128)c^2 \right] \sum_1 EI_{\text{str}_t} (\phi_t)^2 \quad (15)$$

The strain energy stored in the stringers because of torsion is:

$$U_t = (1/2) \sum_1 GC \int_0^L (1/r)^2 (\partial^2 w_r / \partial x \partial \phi)^2 dx \quad (16)$$

and again the summation is extended over all the stringers involved in the bulge in one-half of the cylinder. In this equation $(1/r)(\partial^2 w_r / \partial x \partial \phi)$ is the unit angle of twist for the stringers. In the expression for the Saint Venant torsional rigidity

$$C = 0.14h^4 \quad (16a)$$

since the test specimens were provided with square section stringers of edge length h . Differentiation gives:

$$\partial^2 w_r / \partial x \partial \phi = (\partial / \partial x) \left[\sin^2(\pi x/L) + c \sin^6(\pi x/L) \right] \phi_r' \quad (17)$$

where

$$\begin{aligned} \phi_r' = a_0 n [& -a \sin n\varphi - (3.2a - 3.6)\sin 2n\varphi - (1.8a - 2.4)\sin 3n\varphi + \\ & b \cos n\varphi + (6.4b + 7.2\pi)\cos 2n\varphi + (5.4b + 7.2\pi)\cos 3n\varphi] \end{aligned} \quad (17a)$$

This gives for the strain energy of torsion:

$$U_t = (\pi^2 G C / L r^2) \left[(1/4) + (15/32)c + (189/512)c^2 \right] \sum_1 (\phi_r')^2 \quad (18)$$

where the summation is over one-half the cylinder, as before. Since the variation of the torsional rigidity caused by the different amounts of effective width of sheet is small when calculated according to the Saint Venant theory, it was considered permissible to assume GC a constant.

The values of ϕ_r , ϕ_t , and ϕ_r' vary from stringer to stringer. Also I_{str_r} and I_{str_t} vary around the circumference because the effective width to be added to each stringer changes. Therefore the summations indicated in equations (13), (15), and (18) had to be evaluated numerically for each cylinder investigated.

Strain Energy of Shear Stored in Sheet

The shear strain energy per unit volume was taken as one-half the average effective shear modulus multiplied by the square of the average shear strain γ for each panel of sheet. The average shear strain γ was calculated from the relative displacements of the corners of the panel, as shown in figure 3. Then the total strain energy of shear stored in the sheet is:

$$U_{sh} = (1/2) \sum \gamma^2 G_{eff} L_1 t d \quad (19)$$

where $L_1 t d$ is the volume of one panel and the summation extends over all the panels involved in the bulge in one-half the cylinder. The effective shear modulus G_{eff} depends on the geometric and mechanical properties of and the average normal strain in the panel. Its value was taken from the empirical curves established earlier at PIBAL and presented in figure 24 of reference 15.

The average angle of shear γ was calculated from the equation:

$$\begin{aligned} \gamma = & \left(\alpha_r / L_1 \right) \left(w_{r_{i,j}} - w_{r_{i+1,j}} - w_{r_{i,j+1}} + w_{r_{i+1,j+1}} \right) + \\ & \left(|\alpha_t| / L_1 \right) \left(w_{t_{i,j}} + w_{t_{i+1,j}} - w_{t_{i,j+1}} - w_{t_{i+1,j+1}} \right) + \\ & \left(|\alpha_n| d / L_1 \right) \left(w_{n_{i,j}} + w_{n_{i+1,j}} - w_{n_{i,j+1}} - w_{n_{i+1,j+1}} \right) \end{aligned} \quad (20)$$

where the subscript i refers to the circumferential location, and the subscript j , to the axial location of the corners of the panel.

The rotation w_n of the tangent of the ring is given by the relation:

$$w_n = (1/r)(\partial w_r / \partial \varphi) = (1/r)\Phi_r \quad (21)$$

In reference 16 the values of the numerical factors α_r , α_t , and α_n were determined.

$$\left. \begin{aligned} \alpha_r &= d/10r = 2\pi/105 \\ \alpha_t &= -(1/2) \left[1 - 0.01666 \dots (d/r)^2 \right] \\ \alpha_n &= -(r/d)(0.5 + \alpha_t) \end{aligned} \right\} \quad (22)$$

Substitutions yield:

$$U_{sh} = \left(t d G_o / 2 L_1 \right) \sum_{j=0}^m Q_j \sum_{i=0}^{s-1} (G_{eff} / G_o)_{iR_i} \quad (23)$$

where Q is a function of x only, and R , a function of φ only, given by the relations:

$$\begin{aligned} Q = & \left(\left\{ \sin^2 [\pi j / (m+1)] + c \sin^6 [\pi j / (m+1)] \right\} - \left\{ \sin^2 [\pi (j+1) / (m+1)] + \right. \right. \\ & \left. \left. c \sin^6 [\pi (j+1) / (m+1)] \right\} \right)^2 \end{aligned} \quad (24)$$

$$R = a_o^2 \left[\alpha_r (\phi_{r_i} - \phi_{r_{i+1}}) + |\alpha_t| (\phi_{t_i} + \phi_{t_{i+1}}) + \left(|\alpha_n| d/r \right) (\phi_{r_i}' + \phi_{r_{i+1}}') \right]^2 \quad (25)$$

It is possible to get a result in closed form for the summations Q and R but for convenience the summation was performed numerically.

WORK DONE BY EXTERNAL FORCES

It was observed in the experiments described in reference 9 that the stress distribution was not linear in the cutout portion of the cylinder, although the deviations from linearity were not large as a rule. A good approximation to the experimental curves was obtained by assuming a linear force distribution, which is not equivalent to a linear stress distribution because of the varying amounts of effective width of sheet added to the stringer sections. A comparison of the strain distribution calculated on the assumption of linear force distribution with the experimental strains is given in figure 4 of reference 12. The expression used for the calculation of the force acting on the i th stringer is:

$$P_i = P_{cr} \left[\delta/r + \cos (\alpha + 2\pi i/S) \right] / (\delta/r + \cos \alpha) \quad (26)$$

where P_{cr} is the compressive force acting upon the stringer at the edge of the cutout, and δ is the distance of the neutral axis from the horizontal diameter of the cylinder.

Equal and opposite forces are assumed to be acting at the $x = 0$ and $x = L$ ends of each stringer. The distance between the points of application of these forces shortens at buckling. The work done by the forces is equal to the summation of the forces times the shortening of all the stringers involved in the bulge in one-half the cylinder:

$$W = (1/2) \sum_i P_i \int_0^L \left[(\partial w_r / \partial x)^2 + (\partial w_t / \partial x)^2 \right] dx \quad (27)$$

Substitutions and integration give:

$$W = (\pi^2/L) \left[(1/4) + (15/32)c + (189/512)c^2 \right] \sum_i P_i (\phi_r^2 + \phi_t^2)$$

$$W = (\pi^2/L) \left[(1/4) + (15/32)c + (189/512)c^2 \right] P_{cr} \sum_i (P_i/P_{cr}) (\phi_r^2 + \phi_t^2) \quad (28)$$

The summation in the right-hand member of equation (28) was carried out numerically.

ANTISYMMETRIC DEFLECTION PATTERN

The expression chosen to represent the radial deflections that are antisymmetric longitudinally is:

$$w_r = \left\{ \sin(\pi x/L) + e \sin(4\pi x/L) - \left[(1/3) + (2e/3) \right] \sin(6\pi x/L) \right\} \phi_r \quad (29)$$

for

$$0 \leq \phi \leq \pi/n$$

$$0 \leq x \leq L$$

where ϕ_r is given by equation (12). Also,

$$w_r = 0$$

for $\phi > \pi/n$ and/or $x < 0, x > L$. The expression for the tangential deflections, again on the assumption of inextensional deformations, can be obtained from equations (2) and (29) and is given by

$$w_t = \left\{ \sin(2\pi x/L) + e \sin(4\pi x/L) - \left[(1/3) + (2e/3) \right] \sin(6\pi x/L) \right\} \phi_t \quad (30)$$

for

$$0 \leq \varphi \leq \pi/n$$

$$0 \leq x \leq L$$

where Φ_t is given by equation (3a). Also,

$$w_t = 0$$

for $\varphi > \pi/n$ and/or $x < 0, x > L$. These expressions for w_r and w_t must satisfy the boundary conditions at $\varphi = \pi/n$ given in equations (4a) through (4g).

It can be shown that the expressions for w_r and w_t given by equations (29) and (30) satisfy the given boundary conditions for all values of the longitudinal parameter e , as well as the parameters a and b . In addition, it can be verified that equations (29) and (30) satisfy the requirement for antisymmetry in the axial direction, namely,

$$w_r(x) = -w_r(L-x) \quad (31)$$

for any given value of φ .

CALCULATION OF STRAIN ENERGY FOR THE ANTISYMMETRIC

DEFLECTED SHAPE

The strain energies are derived in the same way as those for the symmetric deflected shape. They are listed below with reference to the equations from which they are derived.

Strain Energy Stored in Rings

From equations (8) and (29) the strain energy of bending at the rings involved in the bulge in one-half the cylinder is:

$$U_r = (a_o^2/2r^3)EI_r M \sum_{j=1}^m \left\{ \sin(2\pi j/L) + e \sin(4\pi j/L) - \left[(1/3) + (2e/3) \right] \sin(6\pi j/L) \right\}^2 \quad (32)$$

where M is given in equation (11). The summation is taken over the rings involved in the bulge and was evaluated numerically.

Strain Energy Stored in Stringers

From equations (12) and (29) the strain energy due to radial bending of the stringers is given by

$$U_{\text{str}_r} = (\pi^4/L^3)(40 + 144e + 208e^2) \sum_1 EI_{\text{str}_r} (\phi_r)^2 \quad (33)$$

From equations (14) and (30) the strain energy due to tangential bending of the stringers is

$$U_{\text{str}_t} = (\pi^4/L^3)(40 + 144e + 208e^2) \sum_1 EI_{\text{str}_t} (\phi_t)^2 \quad (34)$$

Equations (16) and (29) give for the strain energy due to torsion of the stringers:

$$U_t = (\pi^2/L)(2 + 4e + 8e^2)(GC/r^2) \sum_1 (\phi_r')^2 \quad (35)$$

where C is given by equation (16a). The summations for all stringer strain energies were evaluated numerically.

Strain Energy of Shear Stored in Sheet

From equations (19), (21), (29), and (30), the strain energy of shear in the sheet is:

$$U_{\text{sh}} = (tdG_o/2L_1) \sum_{j=0}^m Q_j \sum_{i=0}^{s-1} (G_{\text{eff}}/G_o)_i R_i \quad (36)$$

where Q is given by

$$Q = \left(\left\{ \sin [2\pi j/(m+1)] + e \sin [4\pi j/(m+1)] - \right. \right. \\ \left. \left[(1/3) + (2e/3) \right] \sin [6\pi j/(m+1)] \right\} - \left\{ \sin [2\pi(j+1)/(m+1)] + \right. \\ \left. e \sin [4\pi(j+1)/(m+1)] - \left[(1/3) + \right. \right. \\ \left. \left. (2e/3) \right] \sin [6\pi(j+1)/(m+1)] \right\} \right)^2$$

and R is given by equation (25). The summations $\sum Q$ and $\sum R$ were evaluated numerically.

WORK DONE BY EXTERNAL FORCES

From equations (27), (29), and (30) the work done by the external forces is:

$$W = (\pi^2/L)P_{cr}(2 + 4e + 8e^2)\sum_i (P_i/P_{cr})(\phi_r^2 + \phi_t^2) \quad (37)$$

CALCULATION OF BUCKLING LOAD

The buckling condition is

$$U_r + U_{str_r} + U_{str_t} + U_t + U_{sh} = W \quad (38)$$

where the values of the strain energies and the work must be taken from equations (10), (13), (15), (18), (23), and (28) for the longitudinally symmetric buckling shape, or from equations (32), (33), (34), (35), (36), and (37) for the longitudinally antisymmetric buckling shape. Equation (38) was solved for P_{cr} contained in W in the following way.

Integral numbers of s and $(m + 1)$ were chosen for the number of stringer and ring fields included in the bulge. For these values the Φ^2 , M , and R functions reduced to quadratic expressions in a and b . Next P_{cr} was assumed. This permitted the calculation of the effective widths of sheet acting with the stringers, the moments of inertia of the stringers, and the values of the effective shear modulus in the sheet panels.

Finally, a trial value was chosen for the parameter c (for the symmetric deflected shape) or e (for the antisymmetric deflected shape) in the expressions for the longitudinal variation of the buckled shape. All necessary summations were then carried out. Substitution of all the results in equation (38) made it possible to obtain a solution for P_{cr} in the form:

$$P_{cr} = p_1(a,b)/p_2(a,b) \quad (39)$$

where p_1 and p_2 are quadratic expressions in the parameters a and b . Minimizing this expression for P_{cr} with respect to a and b is equivalent to setting

$$p_{cr} = p_1(a,b)/p_2(a,b) = (\partial p_1/\partial a)/(\partial p_2/\partial a) = (\partial p_1/\partial b)/(\partial p_2/\partial b) \quad (40)$$

where the partial differential coefficients of p_1 and p_2 are linear functions of a and b . Equations (40) give three relations between P_{cr} , a , and b , which may be solved by a trial-and-error procedure. With the aid of an assumed value for P_{cr} , a and b were calculated from the linear equations. These values of a and b were then substituted into the original quadratic expressions in equation (39), yielding a calculated value for P_{cr} . This procedure was repeated with new assumptions for P_{cr} until the value calculated was reasonably close to the one assumed. These values of a and b were then substituted in the original expressions for the strain energies, thus reducing the Φ^2 , M , and R functions to quadratic expressions in c or e , depending on which type of deflected shape was under consideration. The necessary summations were carried out again, and substitution of the results in equation (38) gave a solution for P_{cr} in the form

$$P_{cr} = p_3(c)/p_4(c) \quad (41a)$$

or

$$P_{cr} = p_5(e)/p_6(e) \quad (41b)$$

where p_3 and p_4 are quadratic expressions in the parameter c , and p_5 and p_6 are quadratic expressions in the parameter e . Minimizing this expression for P_{cr} with respect to c or e is equivalent to setting

$$P_{cr} = p_3(c)/p_4(c) = (\partial p_3/\partial c)/(\partial p_4/\partial c) \quad (42a)$$

or

$$P_{cr} = p_5(e)/p_6(e) = (\partial p_5/\partial e)/(\partial p_6/\partial e) \quad (42b)$$

where the partial differential coefficients of p_3 and p_4 are linear functions of c , and the partial differential coefficients of p_5 and p_6 are linear functions of e . These equations can be solved by the same trial-and-error procedure that was used to solve equations (40) for a , b , and P_{cr} . If the value of the parameter c (or e) was different from the trial value assumed at the very outset when the parameters a and b were determined, then the new value of c (or e) was substituted in the expressions for the longitudinal variation of the buckled shape and the minimization procedure of equation (40) was

repeated in order to get new values for a and b . The process was continued until the values of all parameters reached reasonably steady values and the value of P_{cr} approached a minimum.

This procedure involving separate minimizations for the longitudinal and circumferential parameters was used because minimization with respect to all the three parameters at the same time would have yielded nonlinear equations in the parameters. It was considered more convenient to repeat the minimizations than to solve the nonlinear equations.

The procedure was carried out for different numbers of ring and stringer fields included in the bulge. The smallest buckling load obtained in this way was considered the true buckling load.

When the value of P_{cr} obtained in these calculations differed materially from that assumed at the outset, the moments of inertia and effective shear modulus had to be calculated again and the entire procedure repeated.

Details of the procedure may be seen from the numerical example given in the appendix.

COMPARISON OF THEORY AND EXPERIMENT

Numerical calculations were carried out to obtain the buckling load, for the axially symmetric deflected shape, of the cylinders shown in figure 4. The buckling load for the axially antisymmetric deflected shape was determined only for cylinder 75. Typical deflected shapes of a ring and stringers are shown in figure 1 and the results of the calculations are given in table 1. The experimental bending moments at buckling were taken from reference 14.

The theoretical buckling loads were consistently higher than the experimental values, and the deviations between theory and experiment seemed to increase systematically with increase in ring size. Comparison of the theoretical buckling loads for axially symmetric and antisymmetric deflected shapes shows that the symmetric shape gave a lower value but the difference was small. This indicates that the assumption of a symmetric shape was closer to the true deflected shape than the assumption of antisymmetry.

The axial wave length predicted by theory was found to be different from the length of the cutout.

Comparison of results obtained with the 45° cutout cylinders of reference 12 with cylinder 72 of this series which has rings of the smallest size shows a decrease in the deviation between theory and experiment from an average value of 33.9 percent to 18.1 percent. It

appears that the assumption of a more complex deflected shape incorporating more free parameters was the cause of this improvement. However, in the case of the heaviest rings, even the present assumptions are not sufficiently general to give a buckling load in reasonable agreement with experiment.

CONCLUSIONS

A strain-energy theory was developed for the general-instability buckling load of reinforced circular monocoque cylinders having a long symmetric cutout on the compression side and subjected to pure bending. When the theory was applied to four test cylinders of the experimental reports, the buckling loads obtained were 18.1, 26.5, 25.6, and 45.1 percent higher than the experimental values. The average deviation was 28.8 percent.

Polytechnic Institute of Brooklyn
Brooklyn, N. Y., July 12, 1948

APPENDIX

NUMERICAL EXAMPLE

In this appendix details of the calculations performed in determining the buckling load for PIBAL cylinder 73 are shown for the case of a longitudinally symmetric deflected shape. The geometric and mechanical properties for this cylinder are:

Sheet thickness, in.	0.012
Radius, r , in.	10
Distance between adjacent rings, L_1 , in.	3.856
Stringer spacing along circumference, d , in.	3.927
Number of stringers in full portion of cylinder, S	16
Angle of cutout, 2α , deg	45
Stringer cross section, in.	3/8 by 3/8
Area of stringer cross section, A , sq in.	0.140625
Torsional rigidity, C , in. ⁴	27.686×10^{-4}
Ring cross section, in.	1/4 by 1/2
Moment of inertia of ring cross section, I_r , in. ⁴	749.364×10^{-6}
Modulus of elasticity, E , psi	10.5×10^6
Shear modulus, $G = G_0$, psi.	3.9×10^6

At the outset, the assumed value of P_{cr} was taken as 5300 pounds. The shift of the neutral axis was calculated to be 1.1452 inches on the basis of a linear force distribution for pure bending. This permits the setting up of the following table which gives the effective width $2w$ of sheet to be added to the stringers, the moments of inertia of the stringer cross sections, the effective shear modulus G_{eff} , and the reduced moduli of elasticity.

$$[\delta = 1.1452; \epsilon_{or} = 3.3 \times 10^{-4}]$$

(1)	(2)	(3)	(4)	(5)	(6)	(7)	(8)	(9)	(10)	(11)	(12)	(13)	(14)
i	P ₁	ϵA	ϵ	A _{eff}	2w	I _{str_r}	I _{str_t}	E _{tan}	E _{red}	i	ϵ	ϵ/ϵ_{or}	G _{eff} /G _o
0	5300	5.048×10^{-4}	33.5×10^{-4}	0.1506	1.281	19.68×10^{-4}	25.0×10^{-4}	9.79×10^6	10.14×10^6	0 + 1/2	29.3×10^{-4}	8.88	0.475
1	4198.9	3.999	25.3	.1582	1.465	21.76	48.0	10.5	10.5	1 + 1/2	20.4	6.18	.497
2	2550.9	2.429	14.8	.1637	1.923	23.32	87.0	10.5	10.5	2 + 1/2	9.0	2.73	.620
3	606.9	.578	3.1	.1878	3.927	23.92	623.0	10.5	10.5	3 + 1/2	-----	----	1.000

In this table, column (1) refers to the stringer station. Column (2) is obtained from equation (26), column (3), by dividing column (2) by $E = 10.5 \times 10^6$ psi. Columns (4), (5), and (6) can be most conveniently filled in through the use of a previously drawn curve of the strain ϵ against the area A_{eff} of stringer and effective width combination. (A curve of this type was used in the present calculations, and was constructed with the aid of the following formula for the effective width:

$$2w = (1/\epsilon)(d/r) \left\{ 0.3t + 1.535 \left[(t/d)(\epsilon_r - 0.3t)r^{1/2} \right]^{2/3} \right\} \quad (A1)$$

derived in reference 1.)

Columns (7) and (8) give the moments of inertia of the stringers plus their effective width of a curved sheet calculated from the equations:

$$I_{str_r} = (h^4/12) + \frac{\left\{ (h+t)/2 - [(2w)^2/24r] \right\}^2}{(1/2wt) + (1/A)} + 0.8 \left[(2w)^2/24r \right]^2 2wt \quad (A2)$$

$$I_{str_t} = (h^4/12) + (1/12)(2w)^3 t \quad (A3)$$

where h is the width of the stringer. These equations were also derived in reference 1.

If the strain in the stringer is above the proportional limit, it is necessary to use the von Kármán reduced modulus of elasticity for calculating the bending rigidity of the stringers. Columns (9) and (10) give the values of the reduced moduli based on the curves of reference 17.

Column (12) gives the value of the strain in the middle of each panel from which the effective shear modulus can be determined. On the basis of a buckling strain of the panels $\epsilon_{cr} = 3.3 \times 10^{-4}$, column (13) gives the ratio ϵ/ϵ_{cr} for each panel. The values of G_{eff}/G_0 in column (14) are obtained from figure 24 of reference 15.

For the evaluation of the Φ^2 , M , and R functions, the number s of stringer fields included in the bulge in one-half the cylinder was assumed to be four. The corresponding value at n can be obtained from equation (A1):

$$n = S/2s \quad (A4)$$

Only integral numbers of stringer fields were used in the summations, so that the angle ϕ was replaced by its equivalent $(2\pi i/S)$, where $(2\pi/S)$ is the angle subtended by one stringer field, and $i = 1, 2, 3, \dots$ denotes the circumferential location of each stringer. The trigonometric functions appearing in the expressions for Φ_r , Φ_t , and Φ_r' are given in the following table, together with the coefficients of the trigonometric functions.

$$[s = 4; n = 2]$$

i	Constant	$n\phi = \frac{\pi i}{s}$	$\cos \frac{\pi i}{s}$	$\cos \frac{2\pi i}{s}$	$\cos \frac{3\pi i}{s}$	$\sin \frac{\pi i}{s}$	$\sin \frac{2\pi i}{s}$	$\sin \frac{3\pi i}{s}$
0	1	0	1	1	1	0	0	0
1	1	0.785398	0.707107	0	-0.707107	0.707107	1	0.707107
2	1	1.570796	0	-1	0	1	0	-1
3	1	2.356194	-0.707107	0	0.707107	0.707107	-1	0.707107
Multiplier for Φ_r	1	0	a	1.6a -1.8	0.6a -0.3a	b	3.2b 3.6	1.8b 2.4
Multiplier for Φ_t	0	-0.5	0.5b	0.8b 0.9	0.3b 0.4	-0.5a	-0.4a 0.45	-0.1a 0.133...
Multiplier for Φ_r'	0	0	2.0b	12.8b 14.4	10.8b 14.4	-2.0a	-6.4a 7.2	-3.6a 4.8

The polynomial ϕ_r for $i = 0$, for example, is obtained by multiplying, column by column, the expressions in the row for $i = 0$ by the multipliers for ϕ_r and adding the resulting products. The results for ϕ_r , ϕ_t , and ϕ_r' are given in the following table.

i	ϕ_r			ϕ_t			ϕ_r'		
0	-1.6	3.2a	0	4.0840705	0	1.6b	90.477868	0	25.6b
1	18.2068803	0.2828428a	5.1798996b	-0.7369949	-0.464264a	0.1414214b	-21.3946536	-10.3598a	-6.2225416b
2	-4.7398224	-1.6a	-0.8b	-3.7461647	-0.4a	-0.8b	-50.0389342	1.6a	-12.8b
3	-5.543958	-0.2828428a	-1.2201004b	-0.6452392	-0.0242642a	-0.1414214b	28.1828808	2.4402008a	6.2225416b

The value of M can be calculated with the value of $n = 2$ corresponding to $s = 4$ and is

$$M = 73562.5088 + 3487.1679a + 37945.9796b + 805.8186a^2 + 4933.8711b^2 + 1151.000ab \quad (A5)$$

The functions $(\phi_{r_i} - \phi_{r_{i+1}})$, $(\phi_{t_i} + \phi_{t_{i+1}})$, and $(\phi_{r_i}' + \phi_{r_{i+1}}')$ needed for the calculation of R can be determined by adding or subtracting the polynomials in adjacent rows for each column of the above table. However, it must be remembered that all ϕ functions are zero at $i = 4$. The results are not given here. For the values of $r = 10$ inches and $d = 3.927$ inches equations (22) give:

$$\left. \begin{aligned} \alpha_r &= 0.03927 \\ \alpha_t &= -0.49871 \\ \alpha_n &= -0.003272 \end{aligned} \right\} \quad (A6)$$

Substitution in equation (25) gives the values of R which are listed in the following table.

$$[\alpha_r = 0.03927; \alpha_t = -0.49871; \alpha_n = -0.003272]$$

1	R		
0	-0.80694216	0.2842619a	-0.6423940b
1	1.2486636	0.5269357a	0.0700127b
2	2.1360358	0.26904896a	0.4457607b
3	0.5765488	0.0263752a	0.1266206b

The ϕ^2 , M , and R functions appear in the strain-energy expressions in quadratic form, but the squares of the polynomials are not given here.

The next step in the calculations is to assume a value of $(m + 1)$, the number of ring fields involved in the failure. The value chosen was $(m + 1) = 10$ and the summations appearing in equations (10) and (23) were evaluated numerically on that basis. These results as well as the quadratic functions of c appearing in the expressions for the strain energy of the stringers and the external work are given in the following table.

$$[(m + 1) = 10]$$

Factor for strain energy of --			
Ring bending	3.750	5.468750c	2.2558595c ²
Stringer bending	1.0	1.875c	3.4453125c ²
Stringer torsion	0.25	0.46875c	0.3691406c ²
Sheet shear	0.4774575	0.8952328c	0.6753475c ²
External work	0.25	0.46875c	0.3691406c ²

Finally a trial value of the parameter c was chosen. In this numerical example the value of c used is not the original trial value, but one which was obtained after several trials. Substituting the value $c = -1.477$ in the quadratic functions of c makes it possible to evaluate the various strain energies in the form of quadratic expressions in a and b for each value of i .

The quadratic expressions of a and b in Φ^2 , M , and R are multiplied by the following factors from equations (10), (13), (15), (18), (23), and (28), which have been multiplied by $L/a_0^2\pi^2$ for convenience of calculation:

For ring bending:

$$(EI_r L / 2\pi r^3)(3.750 + 5.46875c + 2.2558595c^2) = 9.10990 \quad (A7)$$

For stringer bending:

$$(E\pi^2/L)(1.0 + 1.875c + 3.4453125c^2)(I_{str1}) = 400,399.8I_{str1} \quad (A8)$$

For stringer torsion:

$$(GCr/r^2)(0.25 + 0.46875c + 0.3691406c^2) = 39.16829 \quad (A9)$$

For shear of sheet:

$$\begin{aligned} [G_{otr}(m+1)/\pi S](G_{eff}/G_o)_i(0.4774575 + 0.8952328c + 0.6753475c^2) \\ = 58,482.6(G_{eff}/G_o)_i \end{aligned} \quad (A10)$$

For external work:

$$(P_i/P_{cr})(0.25 + 0.46875c + 0.3691406c^2) = 0.362752(P_i/P_{cr}) \quad (A11)$$

Multiplication of the Φ^2 , M , and R functions by these multipliers and addition of the results make it possible to solve for P_{cr} :

$$P_{cr} = \frac{1,804,446 + 147,812a + 935,431b + 36,451a^2 + 23,960ab + 130,546b^2}{110.0681 + 2.74494a + 61.82786b + 4.27776a^2 + 8.93153b^2 + 1.39202ab} \quad (A12)$$

Differentiation with respect to a and b , respectively, yields:

$$\left. \begin{aligned} P_{cr} &= \frac{147,812 + 23,960b + 72,902a}{2.74494 + 1.39202b + 8.55552a} \\ P_{cr} &= \frac{935,431 + 23,960a + 261.092b}{61.82786 + 1.39202a + 17.86306b} \end{aligned} \right\} \quad (A13)$$

These equations were reduced to two linear equations by assuming a value of $P_{cr} = 5500$ and clearing fractions. The two linear equations were solved simultaneously for a and b :

$$\left. \begin{aligned} a &= -3.019 \\ b &= -3.354 \end{aligned} \right\} \quad (A14)$$

Substitution of these values in equation (A12) gave a value of $P_{cr} = 5507$ pounds. This result was considered sufficiently close to the value assumed originally.

The next step was to substitute these numerical values of a and b into the Φ^2 , M , and R functions in order to allow a minimization with respect to the parameter c . However, the Φ^2 , M , and R functions happened to have been previously evaluated with $a = -3.07$ and $b = -3.36$. Since small changes of the parameters have little effect on the buckling load, and since these values are very close to those given in equations (A14), the latter values were used.

The numerically evaluated Φ^2 , M , and R functions were then multiplied by the remaining factors for the various strain energies from equations (10), (13), (15), (18), (23), and (28), exclusive of the quadratic expressions in c . This gave as multipliers for the c functions:

$$\left. \begin{aligned} \text{For ring bending:} & \quad 161,811.8 \\ \text{For stringer bending:} & \quad 19,103.99 \\ \text{For stringer torsion:} & \quad 123,458.2 \\ \text{For shear of sheet:} & \quad 29,527.52 \\ \text{For external work:} & \quad 136.2066 \end{aligned} \right\} \quad (A15)$$

Multiplication of the quadratic expressions in c by these factors and addition of the results made it possible to solve for P_{cr} as a function of c :

$$P_{cr} = \frac{671,407 + 1,006,057c + 498,239c^2}{34.0517 + 63.8468c + 50.2794c^2} \quad (A16)$$

Differentiation with respect to c as in equation (42a) gives:

$$P_{cr} = \frac{1,006,057 + 996,478c}{63.8468 + 100.5588c} \quad (A17)$$

Assumption of $P_{cr} = 5440$ yields a value of $c = -1.4757$ from equation (A17). Substitution of this value of c in equation (A16) gives $P_{cr} = 5446$. Since this value of c is approximately equal to the trial value $c = -1.477$ assumed at the beginning, the value of P_{cr} obtained is considered the minimum for the number of ring and stringer fields ($s = 4$, $(m + 1) = 10$) under consideration.

The entire procedure was repeated for other integral numbers of ring and stringer fields included in the bulge, and the lowest value of P_{cr} was taken as the minimum value, and hence the value corresponding to the buckling load, for the cylinder.

The final results of the procedure are listed in table 1 for the four cylinders investigated. The cylinders are shown in figure 4.

REFERENCES

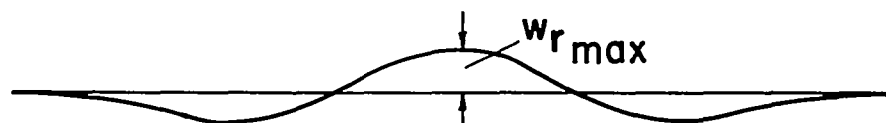
1. Hoff, N. J., and Klein, Bertram: The Inward Bulge Type Buckling of Monocoque Cylinders. I - Calculation of the Effect upon the Buckling Stress of a Compressive Force, a Nonlinear Direct Stress Distribution, and a Shear Force. NACA TN 938, 1944.
2. Hoff, N. J., Fuchs, S. J., and Cirillo, Adam J.: The Inward Bulge Type Buckling of Monocoque Cylinders. II - Experimental Investigation of the Buckling in Combined Bending and Compression. NACA TN 939, 1944.
3. Hoff, N. J., and Klein, Bertram: The Inward Bulge Type Buckling of Monocoque Cylinders. III - Revised Theory Which Considers the Shear Strain Energy. NACA TN 968, 1945.
4. GALCIT: Some Investigations of the General Instability of Stiffened Metal Cylinders. I - Review of Theory and Bibliography. NACA TN 905, 1943.
5. GALCIT: Some Investigations of the General Instability of Stiffened Metal Cylinders. II - Preliminary Tests of Wire-Braced Specimens and Theoretical Studies. NACA TN 906, 1943.
6. GALCIT: Some Investigations of the General Instability of Stiffened Metal Cylinders. III - Continuation of Tests of Wire-Braced Specimens and Preliminary Tests of Sheet-Covered Specimens. NACA TN 907, 1943.
7. GALCIT: Some Investigations of the General Instability of Stiffened Metal Cylinders. IV - Continuation of Tests of Sheet-Covered Specimens and Studies of the Buckling Phenomena of Unstiffened Circular Cylinders. NACA TN 908, 1943.
8. GALCIT: Some Investigations of the General Instability of Stiffened Metal Cylinders. V - Stiffened Metal Cylinders Subjected to Pure Bending. NACA TN 909, 1943.
9. Hoff, N. J., and Boley, Bruno A.: Stresses in and General Instability of Monocoque Cylinders with Cutouts. I - Experimental Investigation of Cylinders with a Symmetric Cutout Subjected to Pure Bending. NACA TN 1013, 1946.
10. Hoff, N. J., Boley, Bruno A., and Klein, Bertram: Stresses in and General Instability of Monocoque Cylinders with Cutouts. II - Calculation of the Stresses in a Cylinder with a Symmetric Cutout. NACA TN 1014, 1946.

11. Hoff, N. J., Boley, Bruno A., and Viggiano, Louis R.: Stresses in and General Instability of Monocoque Cylinders with Cutouts. IV - Pure Bending Tests of Cylinders with Side Cutout. NACA TN 1264, 1948.
12. Hoff, N. J., Boley, Bruno A., and Klein, Bertram: Stresses in and General Instability of Monocoque Cylinders with Cutouts. III - Calculation of the Buckling Load of Cylinders with Symmetric Cutout Subjected to Pure Bending. NACA TN 1263, 1947.
13. Hoff, N. J., Klein, Bertram, and Boley, Bruno A.: Stresses in and General Instability of Monocoque Cylinders with Cutouts. VI - Calculation of the Buckling Load of Cylinders with Side Cutout Subjected to Pure Bending. NACA TN 1436, 1948.
14. Hoff, N. J., Boley, Bruno A., and Mele, Joseph J.: Stresses in and General Instability of Monocoque Cylinders with Cutouts. VII - Experimental Investigation of Cylinders Having Either Long Bottom Cutouts or Series of Side Cutouts. NACA TN 1962, 1949.
15. Hoff, N. J., and Boley, Bruno A.: The Shear Rigidity of Curved Panels under Compression. NACA TN 1090, 1946.
16. Hoff, N. J., Klein, Bertram, and Libby, Paul A.: Numerical Procedures for the Calculation of the Stresses in Monocoques. IV - Influence Coefficients of Curved Bars for Distortions in Their Own Plane. NACA TN 999, 1946.
17. Templin, R. L., Hartmann, E. C., and Paul, D. A.: Typical Tensile and Compressive Stress-Strain Curves for Aluminum Alloy 24S-T, Alclad 24S-T, 24S-RT, and Alclad 24S-RT Products. Tech. Paper No. 6, Aluminum Research Labs., Aluminum Co. of Am., 1942.

TABLE 1
RESULTS OF CALCULATIONS

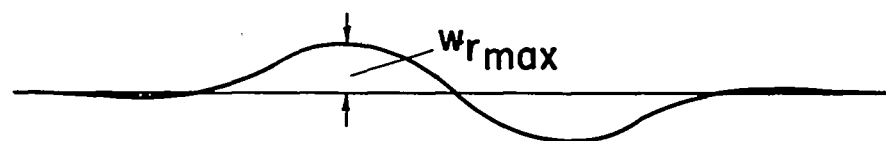
Cylinder	s	n	Ring fields in cutout	(m + 1)	a	b	Axial wave- length parameter, c or e	P _{cr} (lb)	M _{cr} (in.-lb)	M _{exp} (in.-lb)	Deviation, $\frac{M_{cr} - M_{exp}}{M_{exp}} 100$ (percent)
Symmetric deflected shape											
72	4	2	9	7	-2.90	-3.30	0.177	3744	251,000	212,500	18.1
73	4	2	9	10	-3.07	-3.36	-1.476	5446	364,000	287,700	26.5
74	4	2	13	14	-3.07	-3.36	-1.463	6106	406,000	323,200	25.6
75	4	2	13	10	-3.07	-3.36	-1.478	8234	542,000	373,600	45.1
										Average deviation = 28.8 percent	
Antisymmetric deflected shape											
75	4	2	10		-3.07	-3.36	-1.173	8810	584,000	373,600	56.3





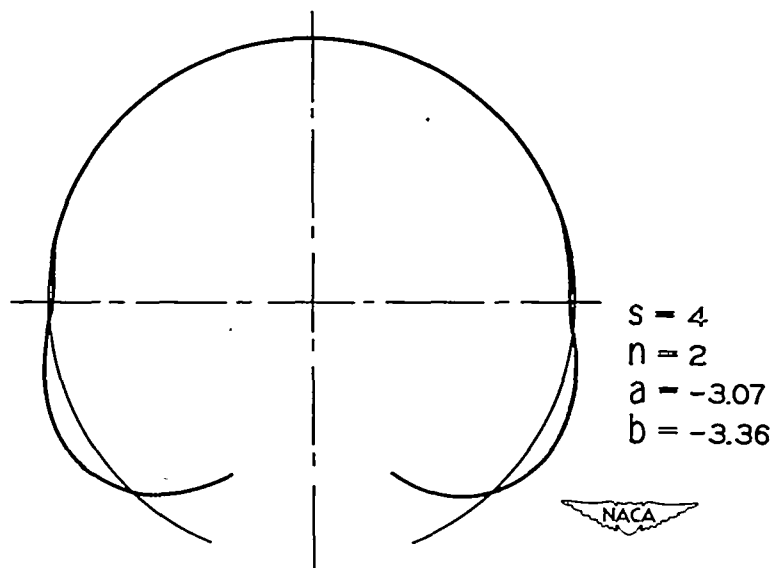
(a) Symmetric deflected shape of a stringer.

$$\sin^2 \frac{\pi x}{L} + C \sin^6 \frac{\pi x}{L}, \quad C = -1.478.$$



(b) Antisymmetric deflected shape of a stringer.

$$\sin \frac{2\pi x}{L} + e \sin \frac{4\pi x}{L} - \left(\frac{1}{3} + \frac{2}{3} e \right) \sin \frac{6\pi x}{L}, \quad e = -1.173.$$



(c) Deflected shape of a ring.

Figure 1.- Deflected shapes of stringers and a ring. Cylinder 75.

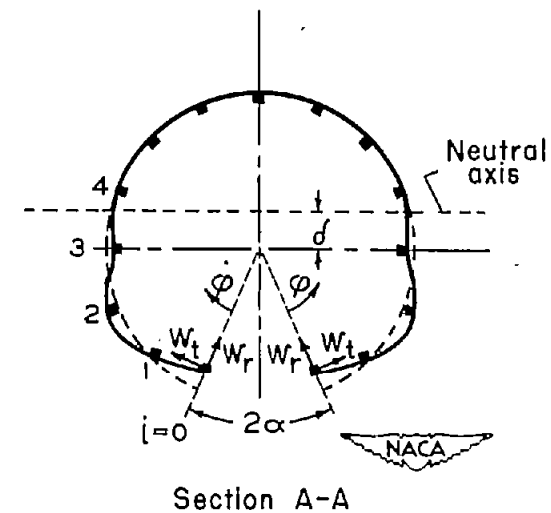
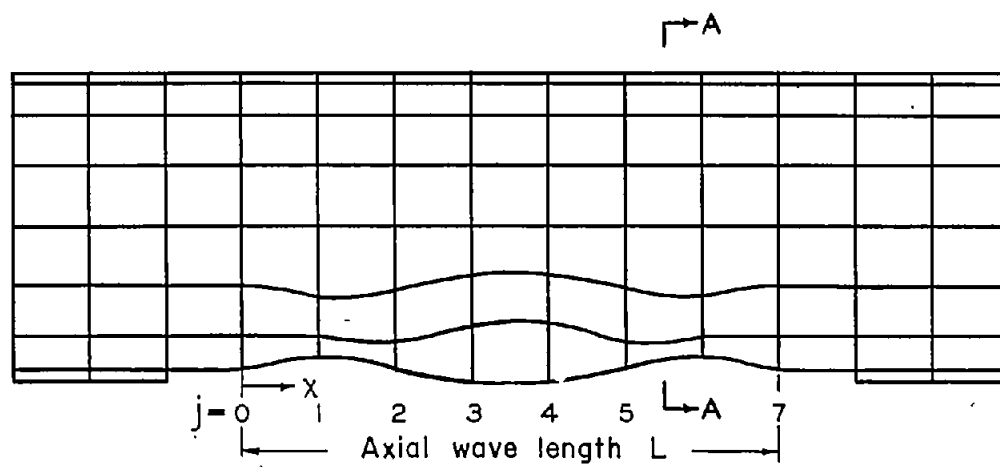


Figure 2.- Sign convention and deflected shape of cylinder.

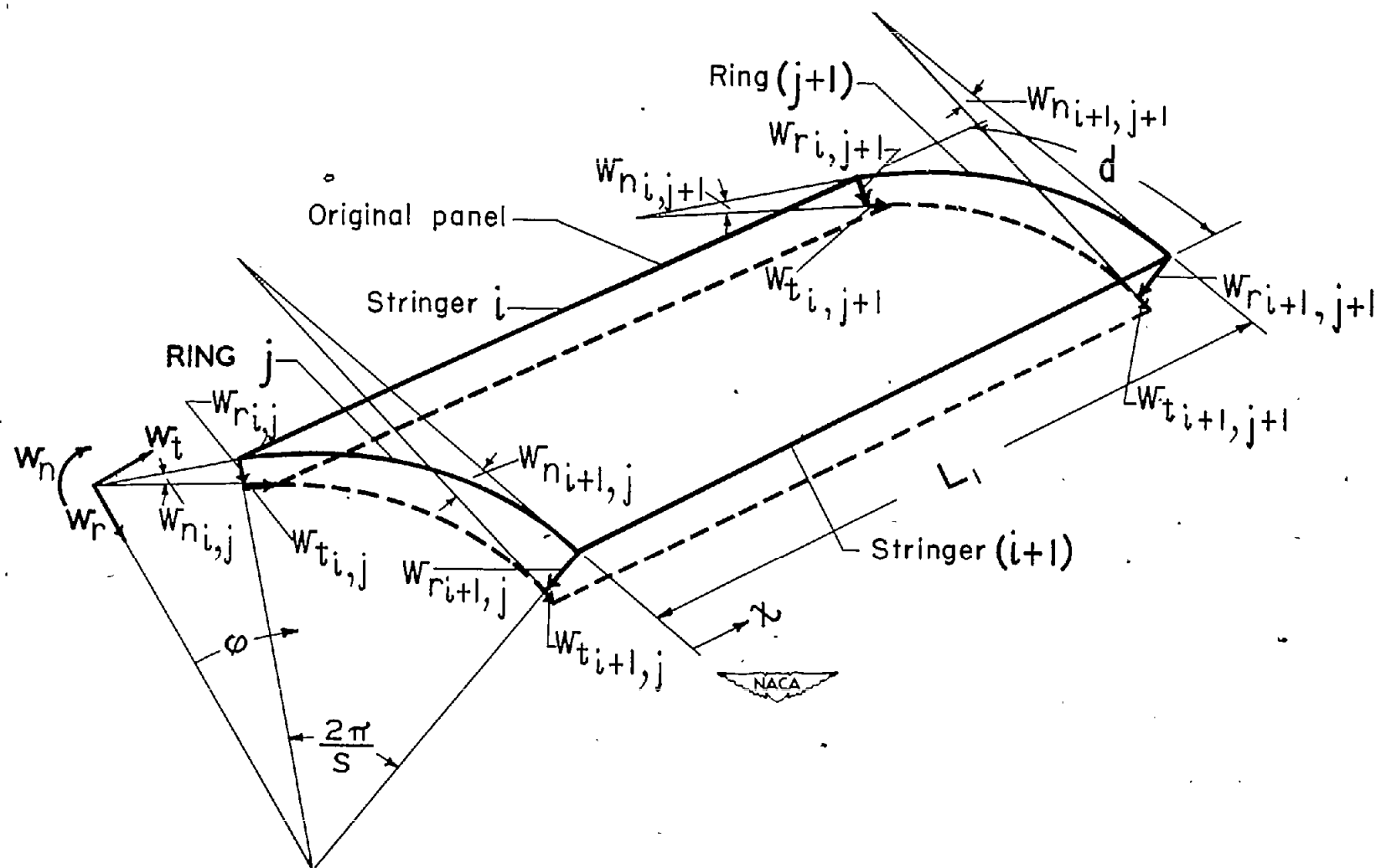


Figure 3.- Notation and sign convention for shear in a panel.

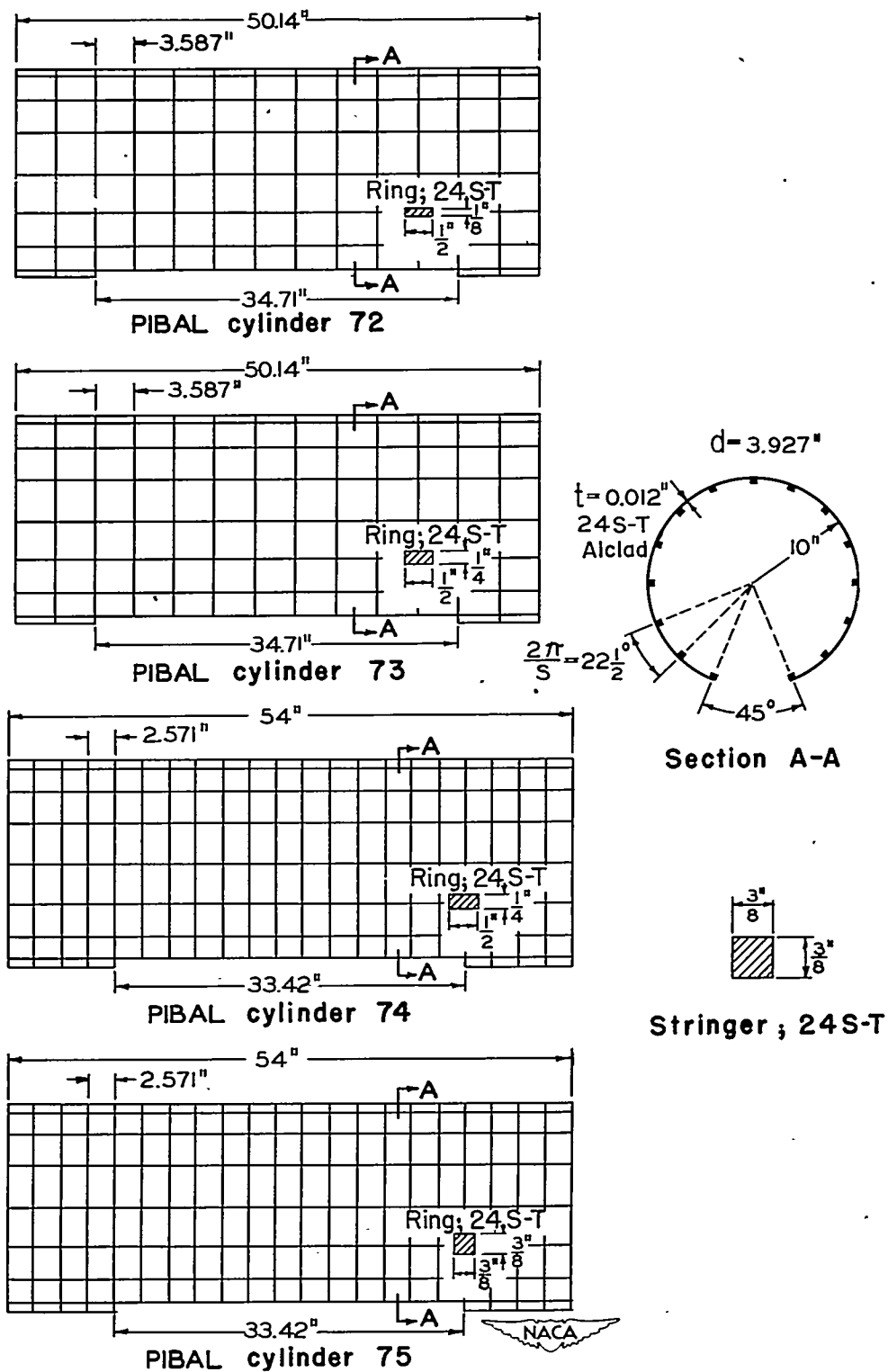


Figure 4.- Monocoque test cylinders.